

# Coupling a discrete state to a quasi-continuum: A model quantum mechanical system that interpolates between Rabi oscillations and decay-revival dynamics

Enes Kutay İŞGÖRÜR<sup>1</sup>, Osman CEVHEROĞLU<sup>2</sup>, Arkadaş ÖZAKIN<sup>2\*</sup>

<sup>1</sup>Department of Physics, Faculty of Engineering, Free University of Berlin, Berlin, Germany

<sup>2</sup>Department of Physics, Faculty of Arts and Sciences, Boğaziçi University, İstanbul, Turkey

---



---

**Abstract:** We formulate a quantum mechanical system consisting of a single discrete state coupled to an infinite ladder of equally-spaced states, the coupling between the two being given by a Lorentzian profile. Various limits of this system correspond to well-known models from quantum optics, namely, the narrow resonance limit gives the Rabi system, the wide resonance limit gives the Bixon-Jortner system, the wide resonance, true continuum limit gives the Wigner-Weisskopf system, and the fixed resonance, true continuum limit gives a system that is typically studied by methods developed by Fano. We give a semi-analytical solution of the eigenvalue problem by reducing it to a transcendental equation, and demonstrate the aforementioned limiting behaviors. We then study the dynamics of the initial discrete state numerically, and show that it gives a wide range of behaviors in various limiting cases as predicted by our asymptotic theory including exponential decay, revivals, Rabi oscillations, and damped oscillations. The ability of this system to interpolate between such a rich set of behaviors and existing model systems, and the accessibility of a semi-analytical solution, make it a useful model system in quantum optics and related fields.

**Key words:** Quantum Mechanics, Quantum Optics, Quantum Revivals, Bixon-Jortner System, Wigner-Weisskopf Solution, Fano Resonances

## 1. Introduction

The two-state system in quantum mechanics is a valuable model whose exact solution is a source of intuition for a wide range of systems in quantum optics, atomic and molecular physics, and even particle physics. The general two-dimensional Hamiltonian is easily diagonalized, giving the dynamics of the system in terms of Rabi oscillations. See [1] for a detailed review of the use of the two-state approximation in the context of atomic physics. Another model system of comparable utility is the so-called Wigner-Weisskopf model where the Hilbert space has a basis consisting of a single discrete state together with a (1-dimensional) continuum of states, with a “flat” coupling between these two pieces. This system can be solved analytically as well, resulting in an instability for the discrete state, whose dynamics being given by an exponential, irreversible decay, with a decay constant which can be obtained exactly from the Fermi golden rule. This decay behavior, as well, comes up in a wide variety of systems, including examples from atomic physics and particle physics. The exact solution in this case was first derived by Wigner and Weisskopf [13], and an elementary derivation is given in [7]. See [2] for a discussion in the context of quantum optics.

These two types of behavior, namely, coherent oscillations of the Rabi system and the irreversible decay of

---

\*Correspondence: arkadas.ozakin@bogazici.edu.tr

the Wigner-Weisskopf system, are two archetypes of quantum evolution, both providing useful approximations in a wide variety of settings.

There are two important generalizations of the Wigner-Weisskopf system which can also be solved analytically or semi-analytically. One generalization, called the Bixon-Jortner system [4], involves replacing the continuum with a quasi-continuum that consists of an infinite set (a “ladder”) of states with a small energy spacing, while still keeping a flat (constant) coupling between the discrete state and the quasi-continuum. In the limit of zero ladder spacing, the behavior of this system converges to that of the Wigner-Weisskopf system, but at finite spacing, the system displays departures from exponential decay such as revivals after an initial decay. Quantum revivals provide a very interesting testground for both theoretical and experimental investigations of quantum behavior (see [5] and [10] for some examples), and the Bixon-Jortner system is one of the simplest settings where one can study such dynamics analytically. The original context where the system was first described was that of quantum chemistry and the problem of “intramolecular radiationless transitions” [4], and thus the BJ system has direct practical use, as well.

The other generalization of the Wigner-Weisskopf system involves keeping the continuum as a real continuum, but choosing a varying coupling coefficient between the discrete state and the continuum, in the sense that the coupling depends on the unperturbed energy eigenvalues of the continuum. Perhaps the most important analytically solvable case consists of using a Lorentzian resonance profile for the coupling as a function of the continuum energy. This generalization results in more complicated (and realistic) behavior, including an analogue of the Lamb shift in eigenvalues, in addition to decay dynamics. In the limit of a wide resonance, one recovers the Weisskopf-Wigner flat coupling behavior, and in the opposite limit of a narrow coupling, one effectively ends up with a coupling to a single state of the continuum, which gives Rabi oscillations for the initial discrete state. See [3] for a derivation using techniques developed by Fano [9] and a detailed discussion.

The two generalizations of the Weisskopf-Wigner system mentioned, namely, the generalization to a non-flat coupling and the generalization to a quasi-continuum, each allow us to cover a richer class of behaviors. For the quasi-continuum, we get revivals in addition to the decay, and for the non-constant (Lorentzian) coupling, we get an analogue of the Lamb shift, and also cover a range of behaviors interpolating between Rabi oscillations and Weisskopf-Wigner decay.

In this paper, we define, and semi-analytically solve, a simultaneous generalization in both of these directions. Namely, we consider a coupling of a discrete state to a **quasi-continuum** as in the Bixon-Jortner system, but we take the **coupling to be non-constant**, as in the Lorentzian generalization of the Weisskopf-Wigner system. This doubly-generalized system interpolates between all four systems described above. By investigating the effects of the tuning parameters, it is possible to obtain the behaviors of the Rabi system, the Bixon-Jortner system, the Wigner-Weisskopf system, and the Lorentzian continuum in appropriate limits. A generic choice of parameters results in a general, much richer range of behaviors.

The rest of the paper is organized as follows. In Section 2, we give a review of the Bixon-Jortner, Rabi, Wigner-Weisskopf, and the Fano/Lorentzian systems. In Section 3, we define our generalization of the BJ system. In Section 4, we derive our solution, and in Section 5, we investigate the properties of the solution by considering various limits. In Section 6, we describe the dynamics of the system when it starts in the discrete state, showing the limiting cases of Rabi oscillations, Fermi golden rule decay, Bixon-Jortner decay-revival dynamics, and the more general behaviors interpolating between these limits. Finally, in Section 7, we discuss our results. Throughout the paper, we work in units where  $\hbar = 1$ .

	Constant Coupling	Lorentzian Coupling
Continuum	Weisskopf–Wigner	“Fano”
Discrete	Bixon–Jortner	?

Table 1: The model systems of quantum optics and our contribution. The generalized, Lorentzian Bixon–Jortner system we study in this paper fills in the question mark.

## 2. Review of relevant systems

In this section, we give a quick review of the Bixon–Jortner, Rabi, and Weisskopf–Wigner systems in order to motivate the generalization we will be pursuing, and to set the notation for the limiting cases we will derive later. For the Bixon–Jortner system, we mostly use the notation of [11].

### 2.1. The Bixon–Jortner system

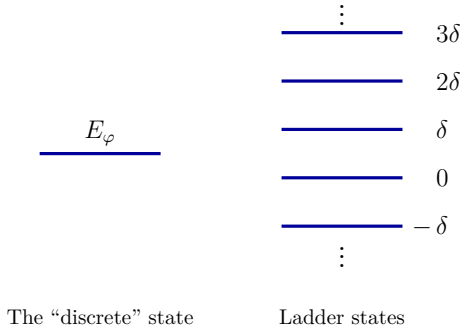


Figure 1: Schematic representation of the unperturbed eigenvalues of the Bixon–Jortner system. The perturbation  $V$  introduces a constant coupling between the discrete state and the ladder.

The Bixon–Jortner system consists of a two-piece Hamiltonian  $H = H_0 + V$  defined on a Hilbert space spanned by the so-called “discrete” state  $|\varphi\rangle$  and a “ladder” (or quasi-continuum) of states  $|n\rangle$ , where  $n = 0, \pm 1, \pm 2, \dots$ . These basis vectors are eigenstates of  $H_0$ :

$$H_0|\varphi\rangle = E_\varphi|\varphi\rangle \quad (2.1)$$

$$H_0|n\rangle = n\delta|n\rangle. \quad (2.2)$$

See Figure 1 for a visual representation. The  $V$  piece of the Hamiltonian couples the discrete state to the quasi-continuum with a constant coupling coefficient  $v$ ,\*

$$\langle n|V|\varphi\rangle = v = \langle \varphi|V|n\rangle \quad (2.3)$$

$$\langle n|V|n\rangle = 0 = \langle \varphi|V|\varphi\rangle. \quad (2.4)$$

\*We will assume  $v$  is real, a complex  $v$  simply adds a phase to the eigenvectors.

The eigenvalues  $E_\mu$  and eigenvectors  $|\psi_\mu\rangle$  of the full Hamiltonian  $H = H_0 + V$  can be found by computing the inner product of the Schrödinger equation  $H|\psi_\mu\rangle = E_\mu|\psi_\mu\rangle$  with  $\langle\varphi|$  and  $\langle n|$ , respectively,

$$\langle\varphi|(H_0 + V)|\psi_\mu\rangle = \langle\varphi|\psi_\mu\rangle E_\mu \quad (2.5)$$

$$\langle n|(H_0 + V)|\psi_\mu\rangle = \langle n|\psi_\mu\rangle E_\mu. \quad (2.6)$$

By inserting a resolution of identity, these give rise to a transcendental equation for the eigenvalues  $E_\mu$ ,

$$\frac{\pi v^2}{\delta} \cot\left(\frac{\pi E_\mu}{\delta}\right) = E_\mu. \quad (2.7)$$

See [11] for a derivation and Figure 3 for a visual representation of the solutions. Making use of the normalization constraint,

$$|\langle\varphi|\psi_\mu\rangle|^2 + \sum_{n=-\infty}^{\infty} |\langle n|\psi_\mu\rangle|^2 = 1, \quad (2.8)$$

and a choice of phase, the components  $\langle\varphi|\psi_\mu\rangle$  and  $\langle k|\psi_\mu\rangle$  of the eigenvectors  $|\psi_\mu\rangle$  can be obtained in terms of the energy eigenvalues as,

$$\langle\varphi|\psi_\mu\rangle = \frac{v}{\left(v^2 + \left(\frac{\Gamma}{2}\right)^2 + E_\mu^2\right)^{1/2}} \quad (2.9)$$

$$\langle k|\psi_\mu\rangle = \left(\frac{v}{E_\mu - k\delta}\right) \langle\varphi|\psi_\mu\rangle, \quad (2.10)$$

where  $\Gamma = \frac{2\pi v^2}{\delta}$ .

The dynamics  $|\psi(t)\rangle$  of the initial state  $|\psi(0)\rangle = |\varphi\rangle$  can be found by using the eigenvector decomposition of  $|\varphi\rangle$ . While the general behavior is rather complex (involving both decays and revivals, as depicted in Figure 7), in the limit of small spacing  $\delta \rightarrow 0$  (taken while keeping  $\Gamma$  constant), one gets an exponential decay given by,

$$|\langle\varphi|\psi(t)\rangle|^2 = e^{-\Gamma t}. \quad (2.11)$$

This is exactly the behavior one would get by using the Fermi golden rule using the density of states  $\rho = 1/\delta$ .

## 2.2. The Rabi system

The Rabi system, or the two-state system is the simplest nontrivial quantum mechanical system. We write its general (time-independent) Hamiltonian as,

$$H = \begin{bmatrix} E_1 & v^* \\ v & E_2 \end{bmatrix} = \alpha_0 I + \alpha \cdot \sigma. \quad (2.12)$$

where  $\sigma = (\sigma_x, \sigma_y, \sigma_z)$  denotes the triple of Pauli matrices, and the real constants  $\alpha_i$ ,  $i = 0, 1, 2, 3$  are given as,

$$\alpha_0 = \frac{E_1 + E_2}{2}, \quad \alpha_3 = \frac{E_1 - E_2}{2}, \quad \alpha_1 + i\alpha_2 = v. \quad (2.13)$$

The two eigenvalues of this Hamiltonian are given as,

$$E_{\pm} = \alpha_0 \pm \sqrt{\alpha_1^2 + \alpha_2^2 + \alpha_3^2} = \left( \frac{E_1 + E_2}{2} \right) \pm \sqrt{\left( \frac{E_1 - E_2}{2} \right)^2 + |v|^2}. \quad (2.14)$$

The corresponding eigenvectors are,

$$|\psi_+\rangle = \begin{bmatrix} \cos(\theta/2)e^{-i\varphi/2} \\ \sin(\theta/2)e^{i\varphi/2} \end{bmatrix}, \quad |\psi_-\rangle = \begin{bmatrix} -\sin(\theta/2)e^{-i\varphi/2} \\ \cos(\theta/2)e^{i\varphi/2} \end{bmatrix}, \quad (2.15)$$

where,

$$\tan \theta = \frac{2|W|}{E_1 - E_2}, \quad v = |v|e^{i\varphi}. \quad (2.16)$$

See [8]. For later reference, we also derive formulas for the special case of  $E_2 = 0$ . In this case, the Hamiltonian is,

$$H = \begin{bmatrix} E_1 & v^* \\ v & 0 \end{bmatrix}, \quad (2.17)$$

and the eigenvalues become,

$$E_{\pm} = \frac{E_1}{2} \pm \sqrt{\frac{E_1^2}{4} + |v|^2}. \quad (2.18)$$

Noting that  $|E_-| = -E_-$  (since  $E_- \leq 0$ ), one gets,

$$\cos \theta/2 = \frac{E_+}{\sqrt{E_+^2 + |v|^2}} = \frac{|W|}{\sqrt{E_-^2 + |v|^2}} \quad (2.19)$$

$$\sin \theta/2 = \frac{|W|}{\sqrt{E_+^2 + |v|^2}} = \frac{-E_-}{\sqrt{E_-^2 + |v|^2}}. \quad (2.20)$$

These formulas allow us to combine the two eigenvector formulas (2.15) into a single formula in terms of the corresponding eigenvalues:

$$|\psi_{\pm}\rangle = \frac{1}{\sqrt{E_{\pm}^2 + |v|^2}} \begin{bmatrix} E_{\pm}e^{-i\varphi/2} \\ |v|e^{i\varphi/2} \end{bmatrix}. \quad (2.21)$$

For the case of a real  $v$  (so that  $\varphi = 0$ ), this becomes,

$$|\psi_{\pm}\rangle = \frac{1}{\sqrt{E_{\pm}^2 + v^2}} \begin{bmatrix} E_{\pm} \\ v \end{bmatrix}. \quad (2.22)$$

Note that these formulas are rather non-standard in that they give the eigenvectors directly in terms of the corresponding eigenvalues.

### 2.3. The Weisskopf-Wigner and Fano solutions

The case of a real continuum of states coupled to a single, “discrete” state can be obtained as the limit of small spacing  $\delta \rightarrow 0$  of a quasi-continuum like the Bixon-Jortner system. One can solve the true continuum case more directly using a technique by Fano [9]. Here we give a quick summary of a specific version that will be relevant to our system.

We assume the Hilbert space of the system is spanned by the discrete state  $|\varphi\rangle$  and a continuum  $|E\rangle$  of states labeled by the unperturbed energy eigenvalue  $E \in \mathbb{R}$ , having Dirac delta normalization,  $\langle E|E' \rangle = \delta(E - E')$ . We assume the total Hamiltonian is given as,

$$H = E_\varphi |\varphi\rangle\langle\varphi| + \int E|E\rangle\langle E|dE + \int v(E) \left[ |E\rangle\langle\varphi|e^{-i\varphi(E)} + |\varphi\rangle\langle E|e^{i\varphi(E)} \right] dE. \quad (2.23)$$

We denote the eigenvectors of the total (perturbed) Hamiltonian as  $|\psi(E')\rangle$ , where  $E'$  denotes the eigenvalue. The eigenvectors can be expanded in terms of the “bare” eigenstates  $|E\rangle$  as,

$$|\psi(E')\rangle = \alpha(E')|\varphi\rangle + \int \beta(E', E)|E\rangle dE. \quad (2.24)$$

Substituting (2.24) and (2.23) in the eigenvalue equation,

$$H|\psi(E')\rangle = E'|\psi(E')\rangle. \quad (2.25)$$

and taking the inner product with  $|\varphi\rangle$  and  $|E\rangle$ , respectively, one gets a set of equations that need to be solved for the coefficients  $\alpha(E')$  and  $\beta(E', E)$ . This procedure gives (see [2] for details),

$$|\alpha(E')|^2 = \frac{W^2(E')}{[E' - F(E') - E_\varphi]^2 + \pi^2 W^4(E')}. \quad (2.26)$$

where  $F(E')$  is given as the principal value integral,

$$F(E') = \mathbb{P} \int \frac{W^2(E)}{E' - E} dE, \quad (2.27)$$

and  $z(E')$  is given as,

$$z(E') = \frac{E' - F(E') - E_\varphi}{W^2(E')}. \quad (2.28)$$

One then obtains  $\beta$  directly in terms of  $\alpha$ . Specializing to the case of  $E_\varphi = 0$ , the Wigner-Weisskopf case is given by a flat (constant) coupling  $W(E) = W$ . For this case one has  $F(E') = 0$ , and with a choice of phase,  $\alpha$  becomes,

$$\alpha(E') = \frac{W}{\sqrt{(E')^2 + \pi^2 W^4}}. \quad (2.29)$$

If instead of a constant coupling, one uses a “resonant coupling”  $W^2(E') = \frac{W^2\gamma}{\pi((E')^2 + \gamma^2)}$  where  $W$  and  $\gamma$  are

constants,<sup>†</sup>  $F(E')$  and  $|\alpha|^2$  become,

$$F(E') = \frac{W^2 E'}{(E')^2 + \gamma^2} \quad (2.30)$$

$$|\alpha(E')|^2 = \frac{W^2 \gamma}{\pi} \frac{1}{[(E')^2 - W^2]^2 + \gamma^2 (E')^2}. \quad (2.31)$$

See [2] for details. If the system is started in the discrete state  $|\varphi\rangle$  at  $t = 0$ , the time evolution can be found by writing  $|\varphi\rangle$  in terms of the energy eigenstates. One gets the probability of finding the system in  $|\varphi\rangle$  at time  $t$  as,

$$P_\varphi(t) = |\langle \varphi | \psi(t) \rangle|^2 = \left| \int |\alpha(E')|^2 e^{-iE't} dE' \right|^2, \quad (2.32)$$

which can be evaluated exactly for the Wigner-Weisskopf case to get the exponential decay behavior predicted by the Fermi golden rule:

$$P_\varphi(t) = e^{-2\pi W^2 t}. \quad (2.33)$$

A similar formula can be derived for the resonant coupling case, which we defer to Section 6.

### 3. Generalizing the Bixon-Jortner system

#### 3.1. The general formalism

We will start with a general system describing a coupling between a discrete state and a quasi-continuum, and will then specialize to the particular case we will investigate. Once again, we use the notation of [11]. Our total Hamiltonian is  $H = H_0 + V$ , where  $H_0$  denotes the unperturbed piece whose eigenvectors consist of an infinite sequence of states  $|k\rangle$  for  $k = 0, \pm 1, \pm 2, \dots$ , and a separate, discrete state  $|\varphi\rangle$ , and  $V$  denotes the coupling between the discrete state and the infinite sequence. As in the Bixon-Jortner system, we will say that the states  $|k\rangle$  form a quasi-continuum or ‘‘ladder’’. In this basis,  $H_0$  is given by,

$$\begin{aligned} H_0|k\rangle &= E_k|k\rangle \\ H_0|\varphi\rangle &= E_\varphi|\varphi\rangle. \end{aligned}$$

The perturbation  $V$  couples the ladder to the discrete state:

$$\begin{aligned} \langle k|V|\varphi\rangle &= v_k = \langle \varphi|V|k\rangle^* \\ \langle k|V|k'\rangle &= 0 \\ \langle \varphi|V|\varphi\rangle &= 0. \end{aligned}$$

Below, we will assume that  $E_k = k\delta$  where  $\delta$  denotes the uniform separation between the ladder states.

We will denote the eigenvalues and the eigenvectors of the full Hamiltonian  $H = H_0 + V$  by  $E_\mu$  and  $|\psi_\mu\rangle$ , respectively:

$$H|\psi_\mu\rangle = E_\mu|\psi_\mu\rangle. \quad (3.1)$$

---

<sup>†</sup>Here we follow the convention of [2], which makes the units of the constant  $W$  different from the units of the  $W$  in the Wigner-Weisskopf case.

To seek these eigenvalues/eigenvectors in terms of those of  $H_0$ , we project Equation (3.1) to  $|\varphi\rangle$  and  $|k\rangle$ , respectively, and use the resolution of identity,

$$I = |\varphi\rangle\langle\varphi| + \sum_k |k\rangle\langle k|.$$

This gives,

$$E_\varphi \langle\varphi|\psi_\mu\rangle + \sum_k v_k^* \langle k|\psi_\mu\rangle = E_\mu \langle\varphi|\psi_\mu\rangle \quad (3.2)$$

$$E_k \langle k|\psi_\mu\rangle + v_k \langle\varphi|\psi_\mu\rangle = E_\mu \langle k|\psi_\mu\rangle, \quad (3.3)$$

respectively, for the two projections. Equation (3.3) gives

$$\langle k|\psi_\mu\rangle = \langle\varphi|\psi_\mu\rangle \frac{v_k}{E_\mu - E_k}, \quad (3.4)$$

and substituting in (3.2), one gets

$$E_\mu = E_\varphi + \sum_k \frac{|v_k|^2}{E_\mu - E_k} \quad (3.5)$$

For given  $k$ -dependent  $E_k$  and  $v_k$ , and a given value for  $E_\varphi$ , solving this equation would give the eigenvalues  $E_\mu$  of the total Hamiltonian  $H$ . We call Equation (3.5) the eigenvalue equation. Using (3.4) and the normalization condition

$$\sum_k |\langle k|\psi_\mu\rangle|^2 + |\langle\varphi|\psi_\mu\rangle|^2 = 1$$

and an overall choice of phase, we get the eigenvectors  $|\psi_\mu\rangle$  in terms of the eigenvalues  $E_\mu$ ,

$$\langle\varphi|\psi_\mu\rangle = \frac{1}{\left[1 + \sum_{k'} \frac{|v_{k'}|^2}{(E_\mu - E_{k'})^2}\right]^{\frac{1}{2}}} \quad (3.6)$$

$$\langle k|\psi_\mu\rangle = \frac{v_k / (E_\mu - E_k)}{\left[1 + \sum_{k'} \frac{|v_{k'}|^2}{(E_\mu - E_{k'})^2}\right]^{\frac{1}{2}}} \quad (3.7)$$

The equations (3.5), (3.6), and (3.7) give us the eigenvalues and the eigenvectors of the coupled Hamiltonian in terms of the eigenvalues and eigenvectors of the uncoupled Hamiltonian and the coupling constants. Of course, obtaining analytic solutions for these is another matter.

### 3.2. The Lorentzian Bixon-Jortner model

In the Bixon-Jortner (BJ) model of Section 2.1, one has  $E_k = k\delta$  and a constant value of the coupling,  $v_k = v$ . Here, we generalize this to a Lorentzian profile with a given resonance width. More explicitly, we make the following choice for the couplings and the unperturbed eigenvalues of the quasi-continuum:

$$\begin{aligned} E_k &= k\delta \\ v_k &= v \frac{\gamma}{\sqrt{\gamma^2 + E_k^2}} = \frac{v}{\sqrt{1 + (\frac{k}{a})^2}}, \end{aligned} \quad (3.8)$$

where  $v$  is a real number,<sup>‡</sup> and  $a = \gamma/\delta$  is a dimensionless variable measuring the width of the coupling  $v_k$  in units of  $\delta$ . See Figure 2 for a visual representation. The quasi-continuum still forms a uniform ladder as in the BJ system, but the coupling now has a peak at  $k = 0$  with dimensionless width  $a$ .

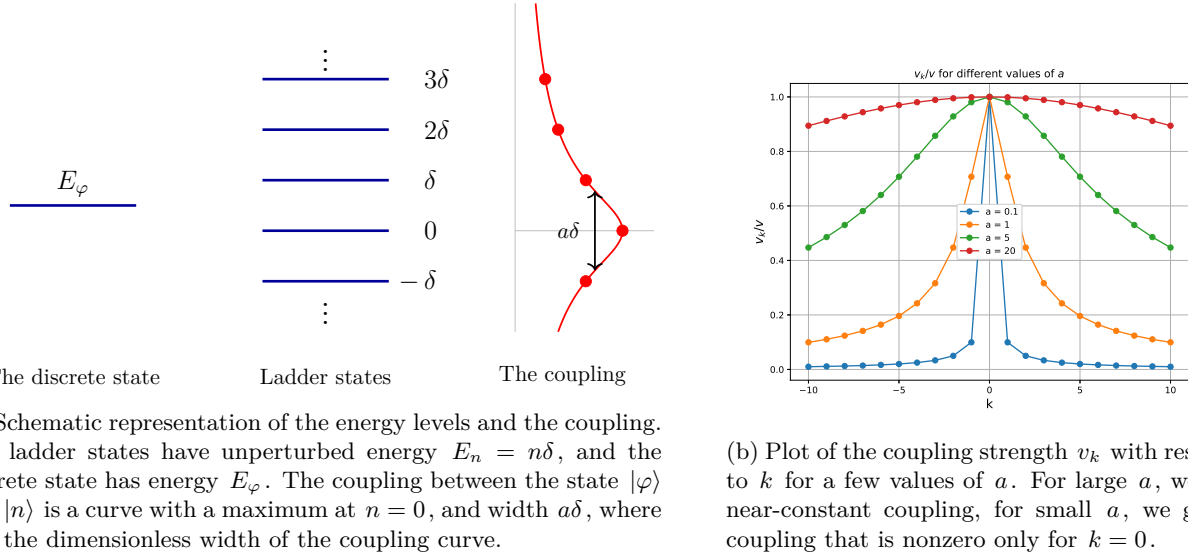


Figure 2: The Lorentzian generalization of the Bixon-Jortner system.

In the limit  $a \rightarrow 0$ , the only ladder state coupled to  $|\varphi\rangle$  will be  $|k=0\rangle$ , all the others getting decoupled. Thus, this limit describes a two-state (Rabi) system with the basis  $|\varphi\rangle$  and  $|k=0\rangle$ , together with a decoupled ladder of states  $|k\rangle$ ,  $k = \pm 1, \pm 2, \dots$ . In the opposite limit of  $a \rightarrow \infty$ , all the couplings get the same value  $v_k = v$ . This is the BJ limit of our system. Thus, the system (3.8) interpolates between the BJ system and the Rabi two-state system (with a decoupled ladder) as the parameter  $a$  is varied between  $\infty$  and 0. Some examples plots of  $v_k$  can be seen in Figure 2.

Another adjustable parameter is the spacing,  $\delta$  (or more appropriately, the dimensionless measure of it  $\delta/v$ ). The limit  $\delta \rightarrow 0$  corresponds to a continuum of energy levels. In the generic case, this gives the Lorentzian continuum reviewed in Section 2.3, and in the case of large  $a$ , it gives the Weisskopf-Wigner model described in the same section. In short, the model (3.8) unifies the Rabi, BJ, Weisskopf-Wigner, and the Lorentzian version of the Fano system, and reduces to these models in special limits.

The time evolution of the Rabi system is known to be oscillatory, whereas when the BJ system is started in the discrete state, it has decays and revivals. The Weisskopf-Wigner system has an exponential decay behavior with the decay rate given exactly by the Fermi golden rule, whereas the Lorentzian Fano system has oscillatory decays. As we will demonstrate in Section 6 the Lorentzian BJ model is rich enough to cover all these behaviors.

<sup>‡</sup>As in the Bixon-Jortner case, a complex generalization is trivial and doesn't bring anything new—the phase of  $v$  comes up only in Equation (3.7).

## 4. The solution

### 4.1. Eigenvalues

Plugging (3.8) into (3.5), we get

$$E_\mu = E_\varphi + \sum_k \frac{v^2}{1 + \frac{k^2}{a^2}} \frac{1}{E_\mu - k\delta} \quad (4.1)$$

Defining the dimensionless forms of the energy eigenvalues  $\epsilon_\mu = E_\mu/\delta$ ,  $\epsilon_\varphi = E_\varphi/\delta$ , we get

$$\epsilon_\mu = \epsilon_\varphi + \frac{v^2}{\delta^2} \sum_k \frac{1}{1 + \frac{k^2}{a^2}} \frac{1}{\epsilon_\mu - k} \quad (4.2)$$

This transcendental equation specifies the energy eigenvalues  $\epsilon_\mu$  of the coupled system. To get a closed form version of (4.2), we need to evaluate the infinite sum

$$S_1(\epsilon_\mu, a) = \sum_{k=-\infty}^{\infty} \frac{1}{1 + \frac{k^2}{a^2}} \frac{1}{\epsilon_\mu - k} \quad (4.3)$$

We accomplish this by using the Mittag-Leffler theorem. Expanding into partial fractions,

$$S_1(\epsilon_\mu, a) = \frac{a^2}{a^2 + \epsilon_\mu^2} \sum_{k=-\infty}^{\infty} \left( \frac{\epsilon_\mu}{a^2 + k^2} + \frac{k}{a^2 + k^2} + \frac{1}{\epsilon_\mu - k} \right) \quad (4.4)$$

Now,  $S_1(\epsilon_\mu, a)$  as defined in (4.3) is absolutely convergent, and we are free to evaluate it using the “principal value” approach of  $\lim_{N \rightarrow \infty} \sum_{k=-N}^N$ . This makes it possible to evaluate (4.4) term by term:

$$S_1(\epsilon_\mu, a) = \frac{a^2}{a^2 + \epsilon_\mu^2} \left[ \lim_{N \rightarrow \infty} \epsilon_\mu \sum_{k=-N}^N \frac{1}{a^2 + k^2} + \lim_{N \rightarrow \infty} \sum_{k=-N}^N \frac{k}{a^2 + k^2} + \lim_{N \rightarrow \infty} \sum_{k=-N}^N \frac{1}{\epsilon_\mu - k} \right] \quad (4.5)$$

The second sum vanishes. The first sum is also absolutely convergent, and is given by

$$\sum_{k=-\infty}^{\infty} \frac{1}{a^2 + k^2} = \frac{\pi}{a} \coth(\pi a) \quad (4.6)$$

The third sum gives,

$$\lim_{N \rightarrow \infty} \sum_{k=-N}^N \frac{1}{\epsilon_\mu - k} = \pi \cot(\pi \epsilon_\mu), \quad (4.7)$$

see, e.g., [6], page 153. Note that this sum also comes up in the Bixon-Jortner model, but it only becomes convergent using the symmetric limit, which means that the infinite BJ system exists only as the limit of a *symmetric* finite ladder. This point is glossed over in [12]. Combining the terms, we get,

$$S_1(\epsilon_\mu, a) = \pi \left[ \frac{\cot(\pi \epsilon_\mu) + \epsilon_\mu \coth(\pi a)/a}{1 + (\epsilon_\mu/a)^2} \right]. \quad (4.8)$$

Substituting this in (4.2), we see that the dimensionless energy eigenvalues  $\epsilon_\mu$  are given by the solutions to the transcendental equation,

$$\epsilon_\mu = \epsilon_\varphi + \frac{\pi v^2}{\delta^2} \left[ \frac{\cot(\pi\epsilon_\mu) + \alpha(a)\epsilon_\mu}{1 + (\epsilon_\mu/a)^2} \right], \quad (4.9)$$

where  $\alpha(a) = \coth(\pi a)/a$  is a term independent of energy. In Figure 3, we show the left hand side (LHS) and the right hand side (RHS) of equation (4.9), together with the RHS of the Bixon-Jortner eigenvalue equation (2.7). See Section 5.4 for further visualization of the eigenvalue equation as the parameters are varied.

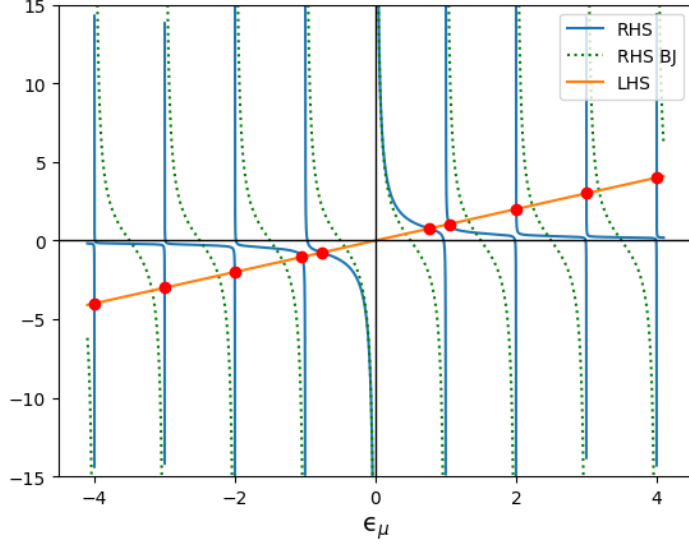


Figure 3: The left hand side (LHS) and the right hand side (RHS) of the transcendental eigenvalue equations (4.9) and (2.7).

#### 4.2. Eigenvectors

We next use (3.6) and (3.7) to obtain the eigenvectors. Once again, working with the dimensionless  $\epsilon_\mu = E_\mu/\delta$ , we have,

$$\langle \varphi | \psi_\mu \rangle = \frac{1}{[1 + \frac{v^2}{\delta^2} S_2(\epsilon_\mu, a)]^{1/2}} \quad (4.10)$$

$$\langle k | \psi_\mu \rangle = \langle \varphi | \psi_\mu \rangle \frac{v_k}{\delta(\epsilon_\mu - k)} \quad (4.11)$$

where

$$S_2(\epsilon_\mu, a) = \sum_{k=-\infty}^{\infty} \frac{1}{1 + (k/a)^2} \frac{1}{(\epsilon_\mu - k)^2}. \quad (4.12)$$

To evaluate this sum, simply note that  $S_2(\epsilon_\mu, a) = -\frac{\partial S_1(\epsilon_\mu, a)}{\partial \epsilon_\mu}$  where  $S_1$  is given in (4.8). Thus,

$$S_2(\epsilon_\mu, a) = \frac{\pi}{1 + (\epsilon_\mu/a)^2} \left[ \pi \csc^2(\pi\epsilon_\mu) - \alpha(a) + \frac{2\epsilon_\mu}{a^2} \frac{\cot(\pi\epsilon_\mu) + \alpha(a)\epsilon_\mu}{1 + (\epsilon_\mu/a)^2} \right], \quad (4.13)$$

where  $\alpha(a) = \coth(\pi a)/a$  as before.

It is also useful to obtain the sum  $S_2(\epsilon_\mu, a)$  and hence the eigenvectors as purely rational functions of  $\epsilon_\mu$ . This can be accomplished by obtaining the cotangent term in (4.13) as a rational function from the eigenvalue equation (4.9). We denote  $\cot \pi \epsilon_\mu$  obtained this way by  $\mathcal{C} = \mathcal{C}(\epsilon_\mu, a)$ , which is given by,

$$\cot \pi \epsilon_\mu = \mathcal{C}(\epsilon_\mu, a) = \frac{\delta^2}{\pi v^2} (1 + (\epsilon_\mu/a)^2) (\epsilon_\mu - \epsilon_\varphi) - \epsilon_\mu \alpha(a) \quad (4.14)$$

Substituting in (4.13), we get

$$S_2(\epsilon_\mu, a) = \frac{\pi}{1 + (\epsilon_\mu/a)^2} \left[ \pi(1 + \mathcal{C}^2) - \alpha(a) + \frac{2\epsilon_\mu}{a^2} \frac{\epsilon_\mu \alpha(a) + \mathcal{C}}{1 + (\epsilon_\mu/a)^2} \right]. \quad (4.15)$$

Note that this is now a rational function of  $\epsilon_\mu$ , which (as opposed to (4.13)), also has an explicit  $v$ -dependence through  $\mathcal{C}$ .

## 5. The behavior of the solution

We next investigate the behavior of the eigenvalues and eigenvectors in various limits. For the original Hamiltonian given by (3.8), the limits we consider are,

1. The  $a \rightarrow \infty$  limit, which makes the system approach the BJ system,
2. The  $a \rightarrow 0$  limit which makes the system approach a two-state (Rabi) system (consisting of  $|0\rangle$  and  $|\varphi\rangle$ ) and a decoupled subsystem (consisting of the remaining  $|n \neq 0\rangle$ ),
3. The  $\delta/v \rightarrow 0$  limit which makes the system approach a true continuum (this limit is taken while keeping  $\Gamma = 2\pi v^2/\delta$  and  $\gamma = a\delta$  constant).

Below, we will make use of the fact that the function  $\alpha(a)$  defined above vanishes in both the small  $a$  and the large  $a$  limit, with the limiting behavior,

$$\alpha(a) = \frac{\coth \pi a}{a} \approx \begin{cases} 1/a & a \rightarrow \infty \\ 1/(\pi a^2) & a \rightarrow 0 \end{cases}. \quad (5.1)$$

### 5.1. The $a \rightarrow \infty$ (BJ) limit

#### 5.1.1. Eigenvalues

Using  $a \rightarrow \infty$  in (4.9), we get

$$\epsilon_\mu \approx \epsilon_\varphi + \frac{\pi v^2}{\delta^2} \cot(\pi \epsilon_\mu) \quad (5.2)$$

As expected, this is precisely the eigenvalue equation (2.7) for the Bixon-Jortner system.

### 5.1.2. Eigenvectors

For  $a \rightarrow \infty$ , using  $\alpha(a) \approx 1/a$  on (4.14) and (4.15), we get

$$\mathcal{C}(\epsilon_\mu, a) \approx \frac{\delta^2}{\pi v^2} (\epsilon_\mu - \epsilon_\varphi) \quad (5.3)$$

$$S_2(\epsilon_\mu, a) \approx \pi^2 \left( 1 + \frac{\delta^4}{\pi^2 v^4} (\epsilon_\mu - \epsilon_\varphi)^2 \right). \quad (5.4)$$

Using (4.10) and (4.11), these give the eigenvectors in this limit as

$$\langle \varphi | \psi_\mu \rangle = \frac{1}{\left[ 1 + \frac{v^2 \pi^2}{\delta^2} + \frac{\delta^2}{v^2} (\epsilon_\mu - \epsilon_\varphi)^2 \right]^{1/2}} \quad (5.5)$$

$$\langle k | \psi_\mu \rangle = \frac{v}{\delta(\epsilon_\mu - k)} \langle \varphi | \psi_\mu \rangle. \quad (5.6)$$

These are exactly the Bixon-Jortner eigenvector formulas (2.9)-(2.10) (see also Equation (17) on page 55 of [11], noting that they use  $E_\varphi = 0$ ).

## 5.2. The $a \rightarrow 0$ (decoupled Rabi) limit

### 5.2.1. Eigenvalues

In the limit  $a \rightarrow 0$ , there are two cases. If  $\epsilon_\mu$  is not close to an integer, then the cotangent term in the eigenvalue equation (4.9) can be ignored and the equation becomes

$$\epsilon_\mu \approx \epsilon_\varphi + \frac{v^2}{\delta^2} \frac{1}{\epsilon_\mu} \quad (5.7)$$

which gives the approximate eigenvalues as

$$\epsilon_{\mu\pm} = \frac{1}{2} \left( \epsilon_\varphi \pm \sqrt{\epsilon_\varphi^2 + 4v^2/\delta^2} \right). \quad (5.8)$$

These are simply the energy eigenvalues of a two-state (Rabi) system with Hamiltonian,

$$H_{\varphi,0} = \begin{bmatrix} \epsilon_\varphi & v/\delta \\ v/\delta & 0 \end{bmatrix}, \quad (5.9)$$

acting on the subspace spanned by the original discrete state  $|\varphi\rangle$  and the single ladder state  $|k=0\rangle$ ; see (2.17). Once again, this is the expected behavior considering the form of the coupling in (3.8)—in the limit  $a \rightarrow 0$ , only the  $k=0$  state is coupled to  $|\varphi\rangle$ .

The remaining set of solutions to the eigenvalue equation (4.9) in the limit  $a \rightarrow 0$  consists of (approximate) nonzero integers. To see how the solutions approach integers in this limit, let  $\epsilon_\mu = n + \Delta$ , with  $\Delta$  small. Then, for  $a \rightarrow 0$ , (4.9) becomes, approximately,

$$n \approx \epsilon_\varphi + \frac{v^2}{\delta^2} \left( \frac{a^2}{n^2 \Delta} + \frac{1}{n} \right) \quad (5.10)$$

whose solution for  $\Delta$  is

$$\Delta = \frac{v^2 a^2}{\delta^2 n^2} \left[ \frac{1}{n - \epsilon_\varphi - v^2/(n\delta^2)} \right] \quad (5.11)$$

which is  $\mathcal{O}(a^2)$  as  $a \rightarrow 0$ . This gives the convergence rate of  $\epsilon_\mu$  to integer values as  $a \rightarrow 0$ .

In short, in the  $a \rightarrow 0$  limit, the system decouples into two pieces: a two-state Rabi system spanned by  $|\varphi\rangle$  and  $|k=0\rangle$ , and a decoupled infinite ladder  $|k\rangle$ ,  $k = \pm 1, \pm 2, \dots$  with a missing step.

### 5.2.2. Eigenvectors

Once again, there are two cases. If  $\epsilon_\mu$  is not close to an integer, its approximate values are given by (5.8), and  $\cot(\pi\epsilon_{\mu\pm})$  and  $\csc(\pi\epsilon_{\mu\pm})$  have the corresponding limiting values. Using  $\alpha(a) \approx 1/(\pi a^2)$  as  $a \rightarrow 0$  and working to lowest order in  $a$ , we get from (4.13),

$$S_2(\epsilon_\mu, a) \approx \frac{1}{\epsilon_\mu^2}, \quad (5.12)$$

which gives the  $|\varphi\rangle$  component of the eigenvectors via (4.10) as

$$\langle \varphi | \psi_\mu \rangle = \frac{1}{\left[ 1 + \frac{v^2}{\delta^2} \frac{1}{\epsilon_\mu^2} \right]^{1/2}}. \quad (5.13)$$

For the  $\langle k | \psi_\mu \rangle$  components, we have from (4.11),

$$\langle k | \psi_\mu \rangle = \frac{v}{\delta(\epsilon_\mu - k) \sqrt{1 + \frac{k^2}{a^2}}} \langle \varphi | \psi_\mu \rangle, \quad (5.14)$$

which gives, as  $a \rightarrow 0$ ,  $\langle k | \psi_\mu \rangle \approx 0$  for  $k \neq 0$  and

$$\langle 0 | \psi_\mu \rangle = \frac{v}{\delta \epsilon_\mu} \frac{1}{\left[ 1 + \frac{v^2}{\delta^2} \frac{1}{\epsilon_\mu^2} \right]^{1/2}}. \quad (5.15)$$

Thus, we get the nonzero components of  $|\psi_\mu\rangle$  as,

$$\langle 0 | \psi_\mu \rangle = \frac{v/\delta}{[\epsilon_\mu^2 + (v/\delta)^2]^{1/2}}, \quad \langle \varphi | \psi_\mu \rangle = \frac{\epsilon_\mu}{[\epsilon_\mu^2 + (v/\delta)^2]^{1/2}}, \quad (5.16)$$

for the case where  $\epsilon_\mu$  is not close to an integer. Using (5.8) for  $\epsilon_\mu = E_\mu/\delta$ , equations (5.16) are precisely the eigenvectors of a two-state Rabi system with a Hamiltonian

$$H_{\text{Rabi}} = \begin{bmatrix} 0 & v/\delta \\ v/\delta & \epsilon_\varphi \end{bmatrix} \quad (5.17)$$

see (2.22). Incidentally, the formulas in (5.16) give a simple representation of the Rabi eigenvectors in terms of the eigenvalues which we hadn't encountered in the literature.

If  $\epsilon_\mu$  is close to an integer,  $\epsilon_\mu = n + \Delta$ , according to (5.11),  $\Delta$  is approximately proportional to  $a^2$ ,  $\Delta \approx \beta a^2$ . Thus we can write  $\cot(\pi\epsilon_\mu) = \cot(\pi n + \pi\Delta) = \cot(\pi\Delta) \approx \frac{1}{\pi\Delta}$ , and similarly for  $\csc^2(\pi\epsilon_\mu)$ , and get,

$$\cot(\pi\epsilon_\mu)^2 \approx \frac{1}{\pi\beta a^2}, \quad \csc^2(\pi\epsilon_\mu) \approx \frac{1}{\pi^2 \beta^2 a^4}. \quad (5.18)$$

These give  $S_2(\epsilon_\mu, a)$  as,

$$S_w(\epsilon_\mu, a) \approx \frac{\pi}{n^2} \frac{1}{\frac{1}{a^2}} \left[ \frac{1}{\pi \beta^2 a^4} - \frac{1}{\pi a^2} \frac{2n \frac{1}{\pi \beta a^2} + \frac{n}{\pi a^2}}{\frac{n^2}{a^2}} \right] \quad (5.19)$$

$$\approx \frac{1}{n^2 \beta^2 a^2}. \quad (5.20)$$

Finally, we get the components of the eigenvector  $|\psi_\mu\rangle$  corresponding to a near-integer eigenvalue  $\epsilon_\mu = n + \Delta$  with  $\Delta \approx \beta a^2$  as,

$$\langle \varphi | \psi_\mu \rangle \approx \frac{1}{\left[ 1 + \frac{v^2}{\delta^2} \frac{1}{n^2 \beta^2 a^2} \right]^{1/2}} \approx 0 \quad (5.21)$$

$$\langle k | \psi_\mu \rangle \approx \frac{v}{\frac{\delta k}{a} (n - k)} \frac{1}{\frac{v}{\delta} \frac{1}{n \beta a}} \approx \begin{cases} 0 & \text{if } k \neq n \\ 1 & \text{if } k = n \end{cases}. \quad (5.22)$$

In short, in the limit  $a \rightarrow 0$ , the eigenvectors corresponding to eigenvalues that are near integers are given approximately by the unperturbed eigenvectors  $|k\rangle$  with  $k = \pm 1, \pm 2, \dots$ , and the remaining eigenvectors are given by a linear combination of  $|\varphi\rangle$  and  $|0\rangle$  the coefficients being given in terms of the appropriate Rabi eigenvectors via (2.22). We emphasize that while the eigenvalues corresponding to  $n \neq 0$  are close to integers  $a \rightarrow 0$  and are thus independent of  $v$ , the eigenvalues in the space spanned by  $|n = 0\rangle$  and  $|\varphi\rangle$  do depend on  $v$  in this limit.

### 5.3. The $\delta \rightarrow 0$ (continuum) limit

In the continuum limit where the spacing  $\delta \rightarrow 0$ , both the original, unperturbed energy eigenvalues  $E_k = \delta k$  and the eigenvalues  $E_\mu$  of the full Hamiltonian become continuous. In order to have a well-defined limiting behavior in this case, we keep the two quantities  $\Gamma = \frac{2\pi v^2}{\delta}$  and  $\gamma = a\delta$  fixed as  $\delta \rightarrow 0$ . This amounts to keeping the decay rate given by the Fermi golden rule approximation and the width of the resonance coupling constant as  $\delta \rightarrow 0$ . Instead of the dimensionless energy values  $\epsilon_\mu$  and  $\epsilon_\varphi$ , in this section we work with their dimensionful versions  $E_\mu = \epsilon_\mu \delta$  and  $E_\varphi = \epsilon_\varphi \delta$ .

We focus on the component  $\langle \varphi | \psi_\mu \rangle$  of the eigenvector  $|\psi_\mu\rangle$ . Via (4.14), we get to lowest order in  $\delta$ ,

$$\mathcal{C} \approx \frac{2}{\Gamma} \left( 1 + \left( \frac{E_\mu}{\gamma} \right)^2 \right) (E_\mu - E_\varphi) - \frac{E_\mu}{\gamma}. \quad (5.23)$$

Substituting this in (4.15) to get  $S_2$  and working once again to lowest order in  $\delta$ , we get,

$$S_2 \approx \frac{\pi^2}{1 + \left( \frac{E_\mu}{\gamma} \right)^2} \left[ 1 + \left( \frac{2}{\Gamma} \left( 1 + \left( \frac{E_\mu}{\gamma} \right)^2 \right) (E_\mu - E_\varphi) - \frac{E_\mu}{\gamma} \right)^2 \right]. \quad (5.24)$$

Finally, substituting in (4.10) and defining  $W^2 = \Gamma\gamma/2$  we get after some manipulation,

$$|\langle \varphi | \psi_\mu \rangle|^2 = \frac{W^2 \gamma}{\pi} \frac{\delta}{(E_\mu(E_\mu - E_\varphi) - W^2)^2 + \gamma^2(E_\mu - E_\varphi)^2}. \quad (5.25)$$

This matches (2.31) in Section 2.3 and formula 6.5.45 in [3]. Note that the remaining  $\delta$  in can either be absorbed in a redefinition (“renormalization”) of the eigenstates  $|\psi_\mu\rangle$  in the continuum limit to get a  $\delta$ -function normalization, or can be explicitly dealt with when summing over  $\mu$ , using  $\sum_\mu f(E_\mu)\delta \rightarrow \int f(E)dE$ . We will follow this latter approach below in our discussion of the decay of the discrete state in this limit.

#### 5.4. Visualization and commentary

In Figure 4, we present a graphical representation of the transcendental eigenvalue equation (4.9) by plotting the two sides of this equation for various parameter settings. Each intersection of these two sides corresponds to an eigenvalue. The figure demonstrates the limiting behaviors we discussed above, where the Rabi, Bixon-Jortner, and decoupled ladder pieces become relevant in specified limits.

### 6. Dynamics of the discrete state

We next investigate the probability  $|\langle\varphi|\psi(t)\rangle|^2$  of finding the system in the discrete state at time  $t$  if we start with the discrete state at  $t = 0$ :  $|\psi(0)\rangle = |\varphi\rangle$ . Using the expansion (4.10) of  $|\varphi\rangle$  in terms of the energy eigenstates, we get the time evolution of  $|\psi(t)\rangle$  via

$$|\psi(t)\rangle = \sum_\mu e^{-iE_\mu t} |\psi_\mu\rangle \langle\psi_\mu|\varphi\rangle, \quad (6.1)$$

where once again we are using units with  $\hbar = 1$ . The probability amplitude for  $|\varphi\rangle$  at time  $t$  is,

$$\langle\varphi|\psi(t)\rangle = \sum_\mu e^{-iE_\mu t} |\langle\varphi|\psi_\mu\rangle|^2 \quad (6.2)$$

$$= \sum_\mu \frac{e^{-iE_\mu t}}{1 + \frac{v^2}{\delta^2} S_2(\epsilon_\mu, a)} \quad (6.3)$$

where we used (4.10) to get  $|\langle\varphi|\psi_\mu\rangle|^2$ .

#### 6.1. The continuum limit

Using (5.25) we get the probability amplitude  $\langle\varphi|\psi(t)\rangle$  as

$$\langle\varphi|\psi(t)\rangle = \delta \sum_\mu \frac{W^2 \gamma}{\pi} \frac{e^{-iE_\mu t}}{(E_\mu(E_\mu - E_\varphi) - W^2)^2 + \gamma^2(E_\mu - E_\varphi)^2} \quad (6.4)$$

As  $\delta \rightarrow 0$ , the sum  $\delta \sum_\mu f(E_\mu)$  becomes the integral<sup>§</sup>  $\int_{-\infty}^{\infty} f(E)dE$ ,

$$\langle\varphi|\psi(t)\rangle = \frac{W^2 \gamma}{\pi} \int_{-\infty}^{\infty} dE \frac{e^{-iEt}}{(E(E - E_\varphi) - W^2)^2 + \gamma^2(E - E_\varphi)^2}. \quad (6.5)$$

Focusing on the case  $E_\varphi = 0$ , we get,

$$\langle\varphi|\psi(t)\rangle = \frac{W^2 \gamma}{\pi} \int_{-\infty}^{\infty} dE \frac{e^{-iEt}}{(E^2 - W^2)^2 + \gamma^2 E^2}. \quad (6.6)$$

<sup>§</sup>For a more detailed justification of this limit, see Appendix A.

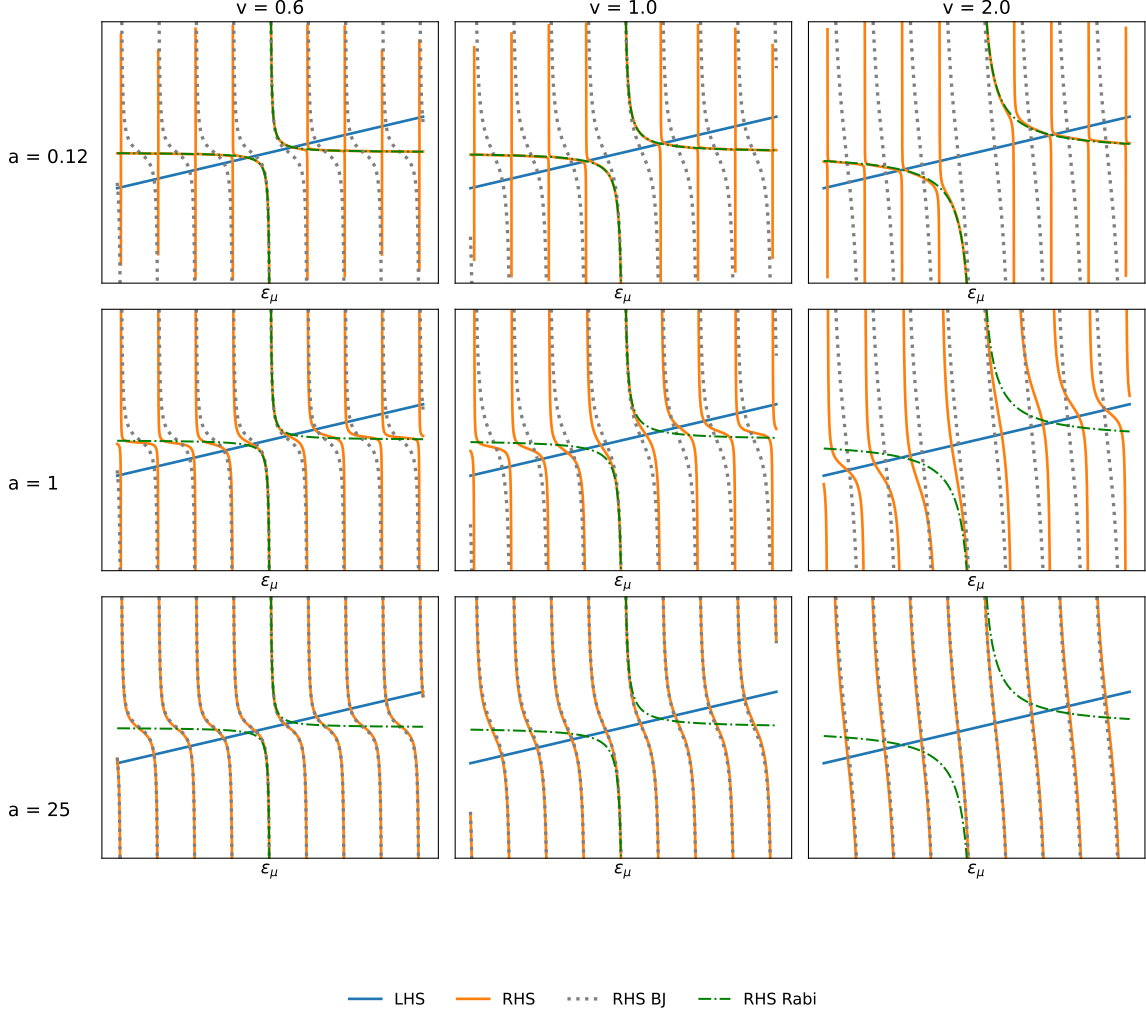


Figure 4: Graphical representation of the transcendental eigenvalue equation (4.9) for different choices of the parameters  $a$  and  $v$ , keeping  $\delta = 1$ . In each plot, the left hand side of the equation is shown in blue and the right hand side is shown in orange. The intersections of these two give the eigenvalues. To compare to the limiting behavior, we also show the RHS of the Bixon-Jortner limit (5.2) in dashed gray, and the Rabi limit (5.8) in dot-dashed green. The top row of three figures have a small value of the dimensionless resonance width  $a$ , hence correspond to the decoupled Rabi limit described in Section 5.2. In this case the eigenvalues are either integers, or the two Rabi values given in (5.8). The solutions in this case lie on either vertical lines or the Rabi curves shown. The bottom three rows have large values of  $a$ , and thus are well-approximated by the Bixon-Jortner case. Thus in this case, the eigenvalues are on the Bixon-Jortner curves. The middle row has intermediate values of  $a$ , and has behavior that is specific to the Lorentzian version of the generalized Bixon-Jortner system. In each row, the three plots correspond to three separate values of the overall coupling scale  $v$ . The case of larger  $v$  corresponds to larger values of  $v/\delta$ , thus approximates the continuum limit.

As expected, this is precisely the same integral that describes the time evolution for the coupling of a discrete state to a true continuum with a Lorentzian coupling, which is covered in detail in, e.g., [3]—see formula 6.5.45 on page 207. The integral (6.6) is evaluated for  $t > 0$  by using contour integration, and one gets,

$$\langle \varphi | \psi(t) \rangle = W^2 \gamma i \left[ \frac{e^{-iE_+ t}}{E_+ [2(E_+^2 - W^2) + \gamma^2]} + \frac{e^{-iE_- t}}{E_- [2(E_-^2 - W^2) + \gamma^2]} \right], \quad (6.7)$$

where,

$$E_{\pm} = \frac{[-i\gamma \pm \sqrt{(4W^2 - \gamma^2)}]}{2}. \quad (6.8)$$

The probability of finding the system in state  $|\varphi\rangle$  is thus (see equation 6.5.47 in [3]),

$$|\langle \varphi | \psi(t) \rangle|^2 = W^4 \gamma^2 \left| \frac{e^{-iE_+ t}}{E_+ [2(E_+^2 - W^2) + \gamma^2]} + \frac{e^{-iE_- t}}{E_- [2(E_-^2 - W^2) + \gamma^2]} \right|^2. \quad (6.9)$$

## 6.2. Visualization and commentary

We next show the dynamics of the generalized (Lorentzian) BJ system starting in the discrete state using various parameter settings, and compare the behavior to known behavior of limiting cases. For plotting the limiting cases, we use the analytical formulas for each limit. For plotting the dynamics of the full system, we use a numerical approach where we form a matrix version of the Hamiltonian (3.8) using  $602 \times 602$  matrices (i.e., using 601 ladder states going from  $n = -300$  to  $n = 300$ , together with the discrete state), obtain the eigenvalues and eigenvectors numerically in Python's NumPy package, and use the formula (6.3) to obtain the dynamics.

In Figures 5 and 6 we show the probability  $|\langle \varphi | \psi(t) \rangle|^2$  as a function of time for the generalized BJ system, using parameters settings that correspond to Figures 2.4 and 2.5 in [2]. We superimpose three plots on top of the generalized BJ dynamics to show how the generalized system interpolates between different types of behavior. Namely, we show,

- The time dependence as given by the exact solution of the BJ system (see Equation 2.5.8 in [2])<sup>¶</sup>
- The Rabi oscillations as given by the corresponding Rabi eigenvalues (2.18)
- An exponential decay whose rate is given by the Fermi golden rule.

As can be seen, in both figures, the dynamics of the generalized BJ system interpolates between Rabi oscillations and the pure BJ decay-revival dynamics. The sharp transitions that happen at  $t = n\delta$  for the BJ system are smoothed by the generalized BJ system.

In Figures 7, 8, and 9, we demonstrate the approach to the continuum limit by choosing progressively smaller values of  $\delta$ , and superpose the known continuum solution of the dynamics for the continuous Lorentzian coupling from Equation (6.9). Since the parameters that describe the continuum behavior are  $W = \sqrt{\Gamma\gamma/2}$  and  $\Gamma$  (see Equation (6.7)), in order to investigate different types of behavior in the continuum setting we plot the dynamics for different regimes in the  $W - \Gamma$  space.

<sup>¶</sup>This equation contains a sign error as we confirmed with Prof. Barnett via email. The plots here use a corrected version of the formula.

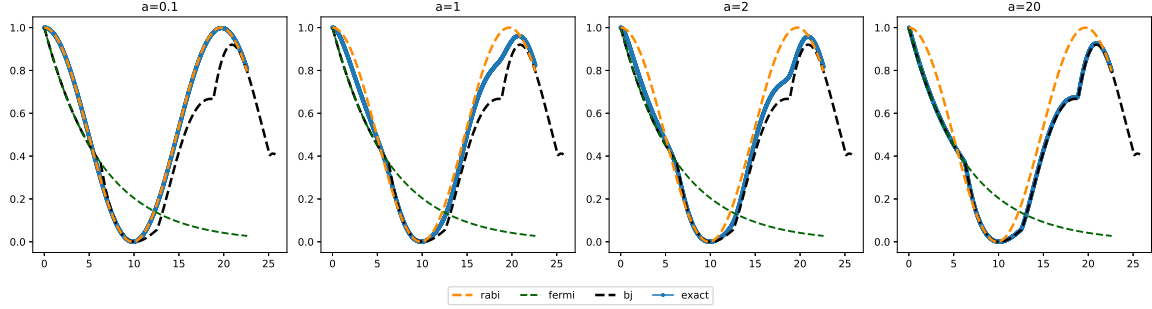


Figure 5: Dynamics of the initial discrete state for different width parameters  $a$ , superposed with pure Rabi oscillations, pure exponential decay, and the Bixon-Jortner decay and revivals. In each plot, the solid blue curves show the dynamics of the generalized BJ-system, and the dashed curves show the superposed limiting systems. These plots correspond to the  $\beta = 0.5$  plot of the BJ system in [2], page 29, which in our notation corresponds to  $v \approx 0.16$ ,  $\delta = 1$ . As  $a$  goes from  $a = 0.1$  to  $a = 20$ , the system behavior interpolates between Rabi oscillations and the BJ revival dynamics given in [2].

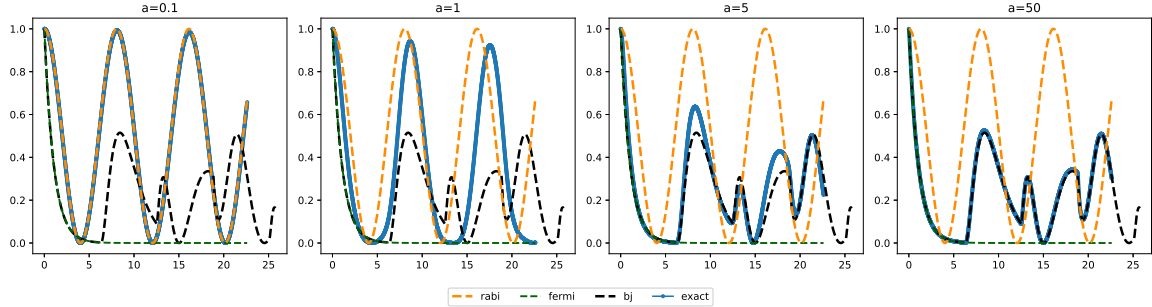


Figure 6: Same as in Figure 5, this time using the Barnett-Radmore setting of  $\beta = 3$ , which in our notation corresponds to  $v \approx 0.39$ ,  $\delta = 1$ . Once again, the behavior interpolates between Rabi oscillations and the BJ revival dynamics as  $a$  is increased.

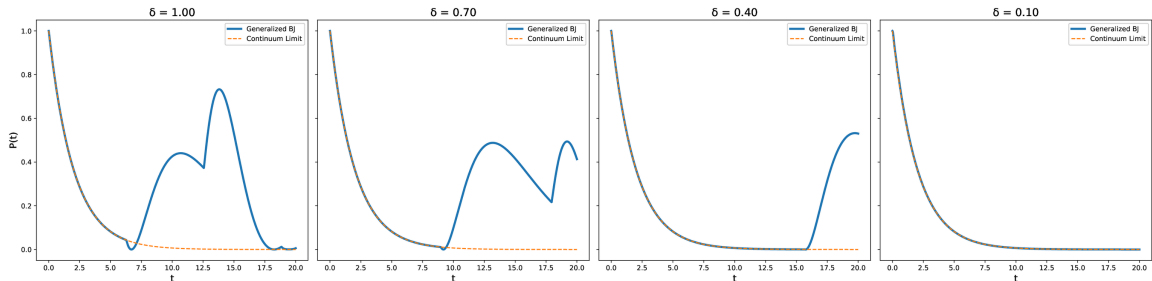


Figure 7: The time dependence of  $|\langle \varphi | \psi(t) \rangle|^2$  for an initial discrete state as one approaches the continuum limit of small  $\delta$ . All plots use the same values for  $W$  and  $\gamma$ , which determine the continuum limit through Equation 6.9. For this set of plots, we have  $W = 8.66$ ,  $\Gamma = 0.5$ , so  $\gamma \gg W$ , which in the continuum limit gives unoscillatory (overdamped) exponential decay.

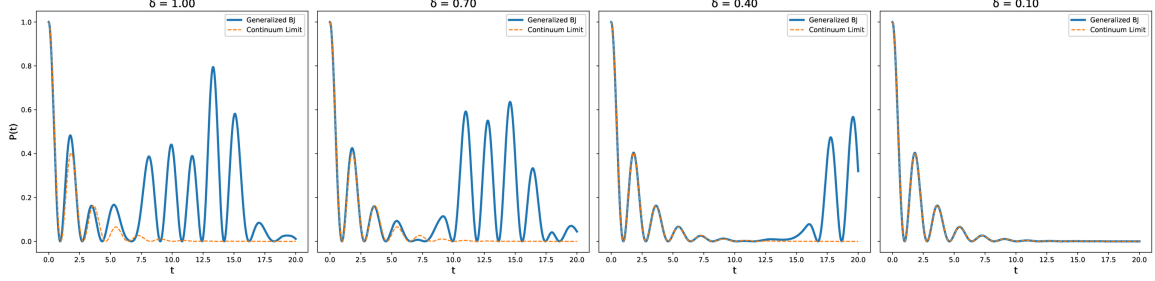


Figure 8: The time dependence of  $|\langle \varphi | \psi(t) \rangle|^2$  for an initial discrete state as one approaches the continuum limit of small  $\delta$ . All plots use the same values for  $W$  and  $\gamma$ , which determine the continuum limit through Equation 6.9. For this set of plots, we have  $W = 1.75$ ,  $\Gamma = 12.25$ , so  $\gamma \ll W$ , which in the continuum limit gives an oscillatory exponential decay.

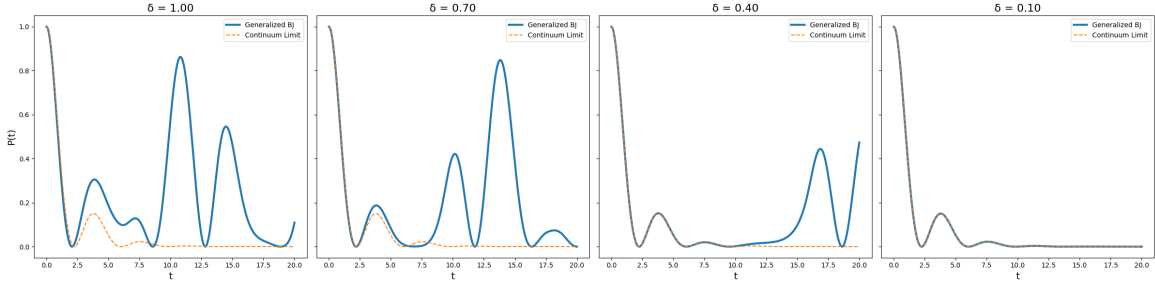


Figure 9: Same as in Figures 7 and 8, this time using an intermediate ratio between  $W$  and  $\gamma$ .  $\Gamma = 3, \gamma = 0.5, W = 0.86, a = (0.5, 0.71, 1, 25, 5), v = (0.69, 0.57, 0.43, 0, 21)$

As discussed in detail by [11], even in the real continuum case, a narrow coupling profile results in approximate Rabi oscillations for an initial discrete state. In Figure 10, we show this approximate behavior by plotting the dynamics in a small  $\delta$  (approximate continuum) setting for smaller and smaller values of the coupling width  $\gamma$ , showing the reduction in decay, approaching true Rabi oscillations.

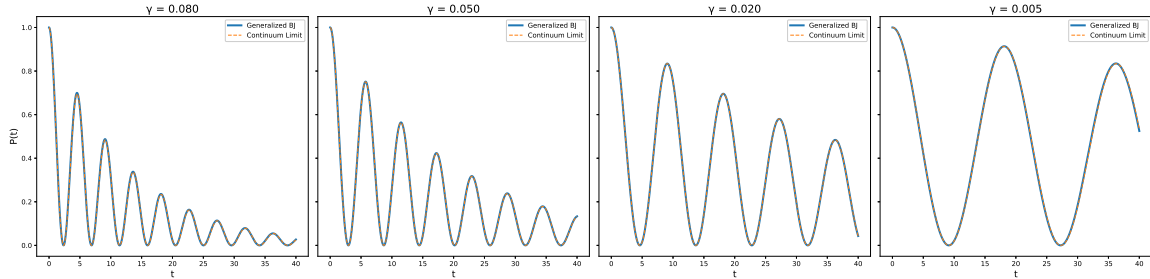


Figure 10: The approach to Rabi oscillations for the generalized BJ system near the continuum limit, which is realized by using a small  $\delta$  (0.005) for all the plots. As the coupling width  $\gamma$  gets small, the decay behavior reduces, making the system approach Rabi oscillations.

## 7. Conclusion

We defined and gave a semi-analytical solution for the diagonalization of a model quantum mechanical system that interpolates between some of the most fundamental prototypes of quantum mechanical behavior. Defined in terms of a ladder of states coupled to a separate, discrete state with a variable coupling, this system approaches the Rabi two-state system in the narrow resonance limit, and the Bixon-Jortner quasi-continuum in the wide resonance limit, covering oscillatory, decay, and revival dynamics as part of these limits. In the quasi-continuum limit of small ladder spacing, the system gives both the Fermi golden rule exponential decay of the Wigner-Weisskopf model, and more general oscillatory decay in the Fano systems investigated in the quantum optics literature. In effect, this system fills in the “missing square” of a  $2 \times 2$  table of model systems given in Table 1.

We hope the wide range of behavior covered and the relatively tractable analytical formulation will allow this system to be of use to researchers and students who depend on model systems to develop understanding and intuition for more complicated systems. Furthermore, we believe this generalized Bixon-Jortner system deserves further studies of its behavior.

**Acknowledgement.** This research was supported in part by Boğaziçi University BAP Program, Project number 20404, project code 25B03D3. We would like to thank Prof. Stephen M. Barnett for helpful communication regarding the dynamics of the Bixon-Jortner discrete state.

## A. Justification of the Integral Limit

During our computation of the time-dependent probability amplitude of the discrete state, we replaced the sum (6.4) with the integral (6.5) in the continuum limit of  $\delta \rightarrow 0$ . While this is a reasonable procedure, one could imagine pathological behavior in the  $\delta \rightarrow 0$  limit where the number of eigenvalues in the interval  $[n\delta, (n+1)\delta]$  depends on  $\delta$  in a complicated way. In this section we show that this pathology does not occur for the generalized BJ system, in the sense that in the  $\delta \rightarrow 0$  limit, there is only a single eigenvalue in each such  $\delta$ -interval.

Let us look at the transcendental equation giving the dimensionless eigenvalues,

$$\epsilon_\mu = \epsilon_\varphi + \frac{\pi v^2}{\delta^2} \left[ \frac{\cot(\pi\epsilon_\mu) + \alpha(a)\epsilon_\mu}{1 + (\epsilon_\mu/a)^2} \right]. \quad (\text{A.1})$$

The dimensionful version written in terms of the constants  $\gamma$  and  $\Gamma$  can be written as

$$g(E_\mu) := E_\varphi + \frac{\Gamma}{2} \left[ \frac{\cot\left(\frac{\pi}{\delta}E_\mu\right) + \frac{\coth\pi a}{\gamma}E_\mu}{1 + (E_\mu/\gamma)^2} \right] - E_\mu = 0. \quad (\text{A.2})$$

Consider the behavior of the function  $g(E_\mu)$  in the interval  $[n\delta, (n+1)\delta]$ :  $g(E_\mu) \rightarrow +\infty$  as  $E_\mu \rightarrow n\delta$  from above, and  $g(E_\mu) \rightarrow -\infty$  as  $E_\mu \rightarrow (n+1)\delta$  from below. Thus if we can show that  $g(E_\mu)$  is strictly decreasing in this interval, it will follow that it has a single root in this interval. Now,  $E_\varphi$  is constant and  $-E_\mu$  is strictly decreasing, thus we only need to show that

$$\frac{\cot\left(\frac{\pi}{\delta}E_\mu\right) + \frac{\coth\pi a}{\gamma}E_\mu}{1 + (E_\mu/\gamma)^2} \quad (\text{A.3})$$

is strictly decreasing. But since  $\frac{1}{1+(E_\mu/\gamma)^2}$  is also decreasing, if we can show that the function

$$f(E_\mu) = \cot\left(\frac{\pi}{\delta}E_\mu\right) + \frac{\coth\pi a}{\gamma}E_\mu \quad (\text{A.4})$$

is strictly decreasing, we are done. Now, the derivative

$$f'(E_\mu) = -\frac{\pi}{\delta} \frac{1}{\sin^2\left(\frac{\pi}{\delta}E_\mu\right)} + \frac{\coth\pi a}{\gamma}, \quad (\text{A.5})$$

has a maximum in our interval at  $E_\mu = (n+1/2)\delta$ , therefore if we can show that this maximum is negative, this will imply that  $f(E_\mu)$  is strictly decreasing. This maximum value becomes zero at  $a = a_0$ , where  $a_0$  is a solution of the equation

$$-\frac{\pi}{\delta} + \frac{\coth\pi a_0}{\gamma} = 0, \quad (\text{A.6})$$

i.e.,  $\coth\pi a_0 = \pi a_0$ . Since  $\coth$  is monotonically decreasing for positive values of its argument,  $f'(E_\mu)$  would be guaranteed to be negative if  $a > a_0$ . Now, we take the limit  $\delta \rightarrow 0$  while keeping  $\gamma = a\delta$  constant, so for small enough values of  $\delta$ ,  $a < a_0$  is guaranteed. In other words, for small enough  $\delta$ ,  $f'(E_\mu) < 0$  in our interval and therefore  $g(E_\mu)$  has a single root in  $[n\delta, (n+1)\delta]$ .

## References

- [1] Leslie Allen and Joseph H Eberly. *Optical resonance and two-level atoms*. Courier Corporation, 2012.
- [2] Stephen Barnett and Paul M Radmore. *Methods in theoretical quantum optics*, volume 15. Oxford University Press, 2002.
- [3] Stephen Barnett and Paul M Radmore. Methods in theoretical quantum optics. volume 15, chapter 6.5. Oxford University Press, 2002.

- [4] Mordechai Bixon and Joshua Jortner. Intramolecular radiationless transitions. *The Journal of chemical physics*, 48(2):715–726, 1968.
- [5] Robert Bluhm, Alan Kostelecky, and James Porter. The evolution and revival structure of localized quantum wave packets. *arXiv preprint quant-ph/9510029*, 1995.
- [6] Henri Cartan. *Elementary theory of analytic functions of one or several complex variables*. Courier Corporation, 1995.
- [7] Claude Cohen-Tannoudji, Bernard Diu, and Frank Laloe. Quantum mechanics. volume 2, chapter XIII–C–3–b. New York, NY (United States); John Wiley and Sons Inc., 2nd edition.
- [8] Claude Cohen-Tannoudji, Bernard Diu, and Frank Laloe. Quantum mechanics. volume 1, page 414. New York, NY (United States); John Wiley and Sons Inc., 2nd edition.
- [9] Ugo Fano. Effects of configuration interaction on intensities and phase shifts. *Physical review*, 124(6):1866, 1961.
- [10] NB Narozhny, JJ Sanchez-Mondragon, and JH Eberly. Coherence versus incoherence: Collapse and revival in a simple quantum model. *Physical Review A*, 23(1):236, 1981.
- [11] Claude Cohen Tannoudji, Gilbert Grynberg, and J Dupont-Roe. Atom-photon interactions. 1992.
- [12] Claude Cohen Tannoudji, Gilbert Grynberg, and J Dupont-Roe. Atom-photon interactions. page 53, 1992.
- [13] Victor Weisskopf and Eugene Wigner. Berechnung der natürlichen linienbreite auf grund der diracschen lichttheorie. *Zeitschrift für Physik*, 63(1):54–73, 1930.